

PEG-*b*-PPS Diblock Copolymer Aggregates for Hydrophobic Drug Solubilization and Release: Cyclosporin A as an Example

Diana Velluto,[†] Davide Demurtas,[‡] and Jeffrey A. Hubbell^{*,†}

Institute of Bioengineering and Institute of Chemical Science and Engineering, Ecole Polytechnique Fédérale de Lausanne, CH-1015 Lausanne, Switzerland, and Centre Intégré de Génomique (CIG), University of Lausanne, CH-1015 Lausanne, Switzerland

Received September 22, 2007; Revised Manuscript Received March 26, 2008; Accepted May 2, 2008

Abstract: Micelles formed from amphiphilic block copolymers have been explored in recent years as carriers for hydrophobic drugs. In an aqueous environment, the hydrophobic blocks form the core of the micelle, which can host lipophilic drugs, while the hydrophilic blocks form the corona or outer shell and stabilize the interface between the hydrophobic core and the external medium. In the present work, mesophase behavior and drug encapsulation were explored in the AB block copolymeric amphiphile composed of poly(ethylene glycol) (PEG) as a hydrophile and poly(propylene sulfide) PPS as a hydrophobe, using the immunosuppressive drug cyclosporin A (CsA) as an example of a highly hydrophobic drug. Block copolymers with a degree of polymerization of 44 on the PEG and of 10, 20 and 40 on the PPS respectively (abbreviated as PEG₄₄-*b*-PPS₁₀, PEG₄₄-*b*-PPS₂₀, PEG₄₄-*b*-PPS₄₀) were synthesized and characterized. Drug-loaded polymeric micelles were obtained by the cosolvent displacement method as well as the remarkably simple method of dispersing the warm polymer melt, with drug dissolved therein, in warm water. Effective drug solubility up to 2 mg/mL in aqueous media was facilitated by the PEG-*b*-PPS micelles, with loading levels up to 19% w/w being achieved. Release was burst-free and sustained over periods of 9–12 days. These micelles demonstrate interesting solubilization characteristics, due to the low glass transition temperature, highly hydrophobic nature, and good solvent properties of the PPS block.

Keywords: Polymer micelle; block copolymer; nanoparticle; poly(propylene sulfide); cyclosporin A

Introduction

There exists an ongoing need for advanced formulations to solubilize and release poorly water-soluble drugs. One such drug, the example of study in this work, is cyclosporin A (CsA), a hydrophobic neutral cyclic peptide consisting of 11 amino acids, 7 of which are N-methylated (Figure 1). CsA contains 4 intramolecular hydrogen bonds, which

imparts a high level of rigidity to its cyclic structure.¹ These molecular features contribute to the low solubility of the molecule in water.

Two oral formulations of the drug are currently available: an oil-based suspension of CsA and a microemulsion that disperses in the gut more rapidly, leading to increased and more reproducible absorption.² An intravenous formulation is also available, employing Cremophor EL, a polyethoxy-

* To whom correspondence should be addressed. Mailing address: Ecole Polytechnique Fédérale de Lausanne, Institute of Bioengineering, LMRP, Mail Station 15, CH-1015 Lausanne, Switzerland. E-mail: jeffrey.hubbell@epfl.ch. Fax: +41 21 693 9665. Tel: +41 21 693 9681.

[†] Ecole Polytechnique Fédérale de Lausanne.

[‡] University of Lausanne.

- (1) Eltayyar, N.; Mark, A. E.; Vallat, P.; Brunne, R. M.; Testa, B.; Vangunsteren, W. F. Solvent-dependent conformation and hydrogen-bonding capacity of cyclosporine-A - evidence from partition-coefficients and molecular-dynamics simulations. *J. Med. Chem.* **1993**, *36*, 3757–3764.
- (2) Cattaneo, D.; Perico, N.; Remuzzi, G. Generic cyclosporine formulations: More open questions than answers. *Transplant Int.* **2005**, *18*, 371–378.

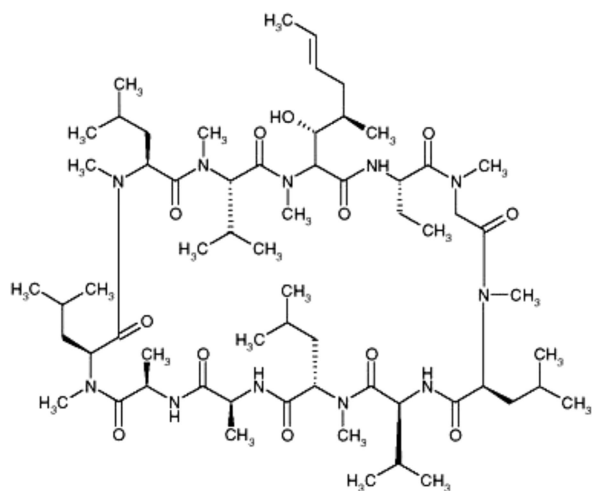


Figure 1. Chemical structure of cyclosporin A, a cyclic undecapeptide of fungal origin.

lated castor oil mainly composed of the glycerol-polyethylene glycol ricinoleate, which is used as a solubilizer and emulsifier. Despite more than 20 years of clinical use, the effectiveness of this potent immunosuppressive drug, as with many other emerging drugs, is still restricted by its poor water solubility. In this regard, the development of new vehicles that can solubilize hydrophobic therapeutic agents effectively and be safe for human administration is of great importance.

Micelles formed from amphiphilic block copolymers have been explored in recent years as carriers for hydrophobic drugs.³ In an aqueous environment, the hydrophobic blocks of the copolymer form the core of the micelle, while the hydrophilic blocks form the corona or outer shell. The hydrophobic micelle core serves as a microenvironment for the incorporation of hydrophobic drugs, while the corona serves as a stabilizing interface between the hydrophobic core and the external medium.

Polymeric micelles with different core- and shell-forming structures have been developed that can remain intact, retain the drug content and target the encapsulated drug away from sites of drug toxicity and toward diseased sites.^{4–8}

Chemistries that have been utilized for such micelles mainly include block copolymers of poly(ethylene glycol)

(PEG) covalently bound with poly(ϵ -caprolactone),⁹ poly(oxypropylene) (PPO),¹⁰ poly(amino acids),^{11,12} or poly(esters),¹¹ in which PEG has been used as hydrophilic block and the uniqueness associated with the different copolymer systems originates from the choice of the hydrophobic block. The various PEG–hydrophobic block combinations have given rise to a number of micelle systems, which have distinct physicochemical properties and different characteristics important to their suitability as drug carriers. Other hydrophobic-core nanoparticulate delivery forms based on amphiphilic block copolymers have also been presented, including polymer nanoparticles that are stabilized by the presence of PEG on their surface, arising from inclusion of PEG as a copolymer block.^{13–15}

Amphiphilic block copolymers, if made with suitable amphiphilic proportions, can also self-assemble into watery-core vesicles when hydrated. The hydrophobic blocks of each molecule tend to associate with each other to minimize direct exposure to water, whereas the more hydrophilic blocks face inner and outer aqueous phases and thereby delimit the two interfaces of a typical bilayer membrane.⁴ In spite of the watery core, in which hydrophilic drugs may be incorporated, the hydrophobic domain within the membrane can be used to solubilize and retain hydrophobic drugs.^{16,17}

Compared to micelles formed from low molecular weight surfactants, polymeric micelles and vesicles are generally more stable, with remarkably lower critical association concentrations (CACs), and have a slower rate of dissociation after dilution, allowing retention of loaded drugs for a longer period of time and, potentially, achieving higher accumulation of a drug at the target site. This fact brings our attention in this study to polymeric amphiphiles in which the hydro-

- (3) Allen, C.; Maysinger, D.; Eisenberg, A. Nano-engineering block copolymer aggregates for drug delivery. *Colloids Surf., B* **1999**, *16*, 3–27.
- (4) Discher, D. E.; Ahmed, F. Polymersomes. *Annu. Rev. Biomed. Eng.* **2006**, *8*, 323–341.
- (5) Kataoka, K.; Harada, A.; Nagasaki, Y. Block copolymer micelles for drug delivery: Design, characterization and biological significance. *Adv. Drug Delivery Rev.* **2001**, *47*, 113–131.
- (6) Kwon, G. S.; Kataoka, K. Block-copolymer micelles as long-circulating drug vehicles. *Adv. Drug Delivery Rev.* **1995**, *16*, 295–309.
- (7) Nishiyama, N.; Kataoka, K. Nanostructured devices based on block copolymer assemblies for drug delivery: Designing structures for enhanced drug function. *Adv. Polym. Sci.* **2006**, *193*, 67–101.
- (8) Sokolsky-Papkov, M.; Agashi, K.; Olaye, A.; Shakesheff, K.; Domb, A. J. Polymer carriers for drug delivery in tissue engineering. *Adv. Drug Delivery Rev.* **2007**, *59*, 187–206.

- (9) Aliabadi, H. M.; Mahmud, A.; Sharifabadi, A. D.; Lavasanifar, A. Micelles of methoxy poly(ethylene oxide)-b-poly(ϵ -caprolactone) as vehicles for the solubilization and controlled delivery of cyclosporine A. *J. Controlled Release* **2005**, *104*, 301–311.
- (10) Kabanov, A. V.; Nazarova, I. R.; Astafieva, I. V.; Batrakova, E. V.; Alakhov, V. Y.; Yaroslavov, A. A.; Kabanov, V. A. Micelle formation and solubilization of fluorescent-probes in poly(oxyethylene-b-oxypropylene-b-oxyethylene) solutions. *Macromolecules* **1995**, *28*, 2303–2314.
- (11) Nakanishi, T.; Fukushima, S.; Okamoto, K.; Suzuki, M.; Matsumura, Y.; Yokoyama, M.; Okano, T.; Sakurai, Y.; Kataoka, K. Development of the polymer micelle carrier system for doxorubicin. *J. Controlled Release* **2001**, *74*, 295–302.
- (12) Yasugi, K.; Nagasaki, Y.; Kato, M.; Kataoka, K. Preparation and characterization of polymer micelles from poly(ethylene glycol)-poly(D,L-lactide) block copolymers as potential drug carrier. *J. Controlled Release* **1999**, *62*, 89–100.
- (13) Gref, R.; Minamitake, Y.; Peracchia, M. T.; Trubetskoy, V.; Torchilin, V.; Langer, R. Biodegradable long-circulating polymeric nanospheres. *Science* **1994**, *263*, 1600–1603.
- (14) Lee, J.; Martic, P. A.; Tan, J. S. Protein adsorption on Pluronic copolymer-coated polystyrene particles. *J. Colloid Interface Sci.* **1989**, *131*, 252–266.
- (15) Muller, R. H.; Wallis, K. H.; Troster, S. D.; Kreuter, J. In vitro characterization of poly(methyl-methacrylate) nanoparticles and correlation to their in vivo fate. *J. Controlled Release* **1992**, *20*, 237–246.

philic block consists of PEG and the hydrophobic block is a liquid or at least amorphous and well above its glass transition temperature, reasoning that liquid- or rubbery-core micelles should be capable of much higher drug loadings than glassy or crystalline cores.¹⁸ Moreover, we sought a hydrophobic block liquid or amorphous phase that could serve as a bona fide solvent for the incorporated drug. In particular, we explored AB block copolymers of PEG and poly(propylene sulfide) (PPS), an analogue of the much more explored poly(propylene glycol), making these copolymers analogues of the well-studied Pluronics.^{5,10,19,20} PPS possesses a very low glass transition temperature of 230 K,^{21,22} and at degrees of polymerization (DPs) used in this work it is a liquid. Our group has previously shown that these macroamphiphiles self-assemble into spherical micelles, cylindrical micelles and vesicles, depending on the relative block sizes.²³ We have further shown that the hydrophobic PPS block can be eventually rendered hydrophilic by oxidation to the poly(propylene sulfone),^{21,24,25} allowing a novel mechanism of aggregate destabilization and potential elimination from the body as a low molecular weight soluble polymer.

In the present work we synthesize and characterize a family of PEG-*b*-PPS diblock copolymers, varying the DP of the PPS at constant PEG DP, and we determine the dependence of mesophase morphology and CsA loading (efficiency and amount) and release upon the macroamphiphile architecture. Copolymers were found that permitted loading efficiencies of CsA as high as 66% at loadings as high as 1.9 mg/mL and that released their payload over periods as prolonged as 12 days. Moreover, the copolymers permitted loading either by the cosolvent evaporation method or by simple suspension in hot water at high loading efficiency, demonstrating the versatility and practicality of the PEG-*b*-PPS platform.

Materials and Methods

Materials. Poly(ethylene glycol) monomethyl ether (average molecular weight 2000 g mol⁻¹), propylene sulfide, thionyl bromide, thioacetic acid and CsA were obtained from Fluka (Buchs, Switzerland). Sodium methoxide, 2,2'-dithiopyridine and pyrene were obtained from Aldrich (Steinheim, Germany). All the solvents were purchased from Sigma-Aldrich and were not further purified. THF was used without stabilizers.

Synthesis and Characterization of PEG-*b*-PPS Diblock Copolymers. PEG-*b*-PPS block copolymers were synthesized by anionic ring opening polymerization of propylene sulfide²⁶ (Figure 2A).

PEG Bromide. PEG monomethyl ether (20 g) was dissolved in 300 mL of toluene, evacuated and purged with argon and heated at 140 °C to reflux for 4–5 h. After cooling the solution at room temperature, 2.5 equiv of thionylbromide (25 mmol, 2 mL) was added carefully; the reaction mixture was stirred at 140 °C to reflux overnight. The orange solution obtained was purified by precipitation in diethyl ether to obtain a white powdery compound. The ¹H NMR spectrum of PEG-Br in (CD₃)₂SO, recorded on a Bruker 400 UltraShield spectrometer at room temperature, was used to confirm the 100% conversion of the monohydroxy PEG monomethyl ether to PEG-Br (no evidence of –OH (δ = 6.65 ppm)).

PEG Thioacetate. Five grams of PEG-Br was introduced in a Schlenk tube and dissolved with 50 mL of DMF (previously dehydrated), evacuated and purged with argon. To this, 5 equiv of potassium carbonate (1.67 g; 12.11 mmol) and 5 equiv of thioacetic acid (0.841 mL; 12.11 mmol) were added, and the mixture was stirred at room temperature overnight. After filtration, the solution was treated with activated charcoal and precipitated twice in diethyl ether. A white solid PEG-thioacetate was collected. ¹H NMR (CDCl₃): δ = 2.33 (s, 3H, –SCOCH₃), 3.06–3.11 (t, 2H, –CH₂SCOCH₃), 3.37 (s, 3H, –OCH₃), 3.54–3.58 (t, 2H, –OCH₂CH₂S–), 3.5–3.7 (broad, PEG chain protons) ppm.

PPS Polymerization. One gram of PEG thioacetate was introduced in a Schlenk tube under argon atmosphere and

- (16) Ahmed, F.; Pakunlu, R. I.; Brannan, A.; Bates, F.; Minko, T.; Discher, D. E. Biodegradable polymersomes loaded with both paclitaxel and doxorubicin permeate and shrink tumors, inducing apoptosis in proportion to accumulated drug. *J. Controlled Release* **2006**, *116*, 150–158.
- (17) Ahmed, F.; Pakunlu, R. I.; Srinivas, G.; Brannan, A.; Bates, F.; Klein, M. L.; Minko, T.; Discher, D. E. Shrinkage of a rapidly growing tumor by drug-loaded polymersomes: pH-triggered release through copolymer degradation. *Mol. Pharmaceutics* **2006**, *3*, 340–350.
- (18) Yamamoto, Y.; Yasugi, K.; Harada, A.; Nagasaki, Y.; Kataoka, K. Temperature-related change in the properties relevant to drug delivery of poly(ethylene glycol)-poly(D,L-lactide) block copolymer micelles in aqueous milieu. *J. Controlled Release* **2002**, *82*, 359–371.
- (19) Kabanov, A. V.; Batrakova, E. V.; Alakhov, V. Y. Pluronic block copolymers as novel polymer therapeutics for drug and gene delivery. *J. Controlled Release* **2002**, *82*, 189–212.
- (20) Oh, K. T.; Bronich, T. K.; Kabanov, A. V. Micellar formulations for drug delivery based on mixtures of hydrophobic and hydrophilic Pluronic block copolymers. *J. Controlled Release* **2004**, *94*, 411–422.
- (21) Napoli, A.; Valentini, M.; Tirelli, N.; Muller, M.; Hubbell, J. A. Oxidation-responsive polymeric vesicles. *Nat. Mater.* **2004**, *3*, 183–189.
- (22) Nicol, E.; Nicolai, T.; Durand, D. Dynamics of poly(propylene sulfide) studied by dynamic mechanical measurements and dielectric spectroscopy. *Macromolecules* **1999**, *32*, 7530–7536.
- (23) Napoli, A.; Tirelli, N.; Wehrli, E.; Hubbell, J. A. Lyotropic behavior in water of amphiphilic ABA triblock copolymers based on poly(propylene sulfide) and poly(ethylene glycol). *Langmuir* **2002**, *18*, 8324–8329.
- (24) Napoli, A.; Bermudez, H.; Hubbell, J. A. Interfacial reactivity of block copolymers: Understanding the amphiphile-to-hydrophile transition. *Langmuir* **2005**, *21*, 9149–9153.
- (25) Napoli, A.; Boerakker, M. J.; Tirelli, N.; Nolte, R. J. M.; Sommerdijk, N.; Hubbell, J. A. Glucose-oxidase based self-destructing polymeric vesicles. *Langmuir* **2004**, *20*, 3487–3491.

- (26) Napoli, A.; Tirelli, N.; Kilcher, G.; Hubbell, J. A. New synthetic methodologies for amphiphilic multiblock copolymers of ethylene glycol and propylene sulfide. *Macromolecules* **2001**, *34*, 8913–8917.

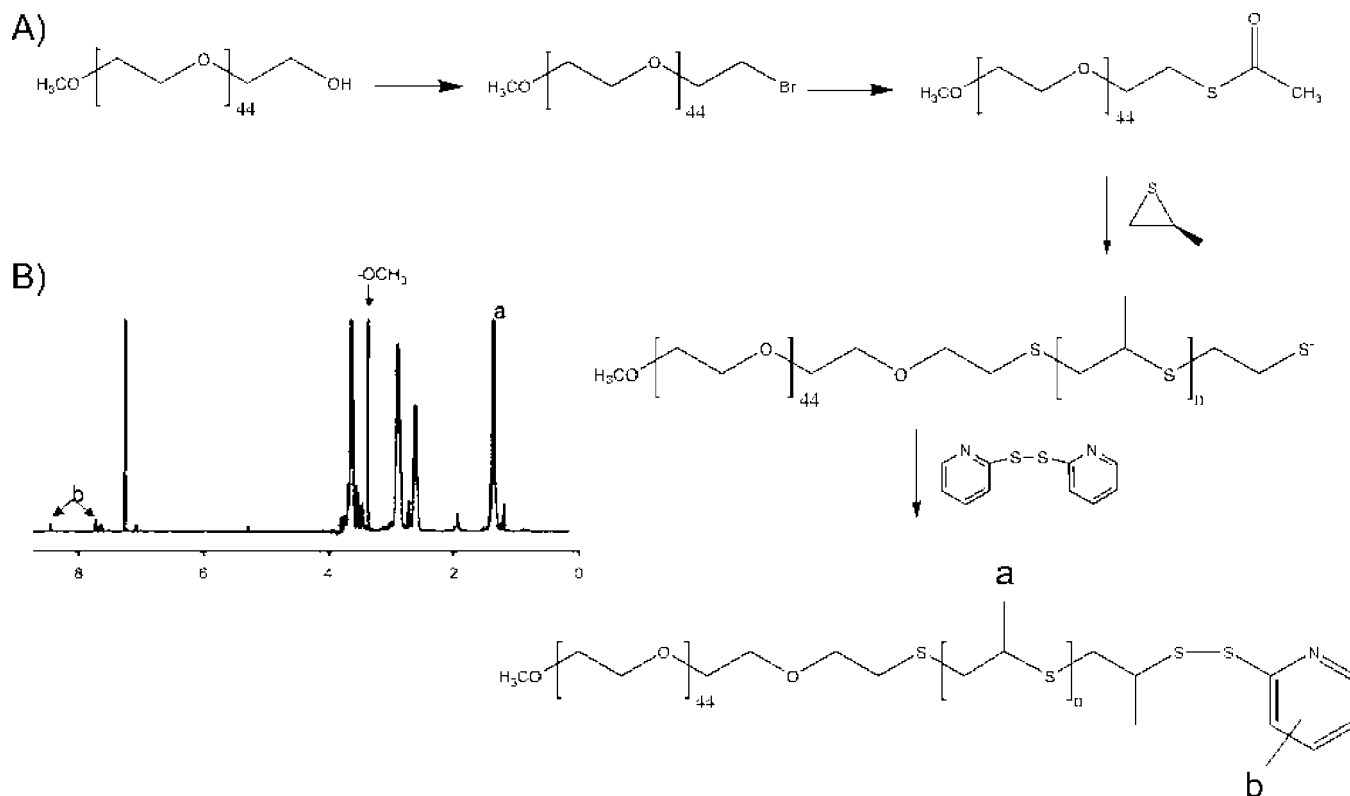


Figure 2. (A) Synthesis scheme. Monomethoxy-PEG₄₄-OH was functionalized to create a protected thiol (thioacetate group) and then deprotected *in situ* to form a thiolate-terminated PEG₄₄-S⁻, which initiated a living anionic ring-opening polymerization of propylene sulfide. The end-capping agent 2,2'-dithiopyridine was added to terminate the polymerization, and PEG₄₄-*b*-PPS_n-SS-pyridine diblock copolymers were obtained. (B) ¹H NMR of a diblock copolymer. A signal from the -OCH₃ group of PEG₄₄ is present at 3.38 ppm and from the -CH₃ group of PPS is present at 1.35–1.45 ppm. The presence of the pyridine end group was assessed by the signal at 7.8–7.83 ppm.

dissolved in THF (1 mL/mg of PEG). To this, 1.1 equiv of sodium methoxide (0.5 M in methanol) was added via syringe, and the mixture was stirred at room temperature for 30 min. After this, a variable amount of propylene sulfide (10, 20 or 40 equiv) was added and incubated for 1 h. An excess of 2,2'-dithiopyridine (440.64 mg, 2 mmol) was finally added as an end-capping agent, and the mixture was stirred at room temperature overnight. The solution was filtered and washed with dichloromethane and precipitated in diethyl ether. ¹H NMR (CDCl₃): δ = 1.35–1.45 (d, CH₃ in PPS chain), 2.6–2.7 (m, CH in PPS chain), 2.85–3.0 (m, CH₂ in PPS chain), 3.38 (s, 3H, -OCH₃), 3.52–3.58 (t, 2H, -OCH₂CH₂S), 3.5–3.7 ppm (broad, PEG chain protons), 7.8–7.83 (m, 1H, pyridine group) (Figure 2B). The degree of polymerization of the PPS block was determined by taking the ratio of PEG protons to PPS protons.

Prepared polymers were characterized for their average molecular weight and polydispersity by gel permeation chromatography (GPC). Samples (20 mL from 10 mg/mL polymer stock solutions in THF) were injected into three serial Waters Styragel HR columns. A 1 mL/min THF mobile phase, set at 40 °C, allowed the detection of the polymer using a differential refractometer detector (model 410, Waters). The calibration curve was prepared using PEG standards (Polymer Laboratories Ltd., U.K.).

Preparation and Characterization of PEG-*b*-PPS

Micelles. Self-assembly of block copolymers was achieved by (a) a cosolvent evaporation method and (b) a hot water suspension method.

(a) Cosolvent evaporation method: PEG-*b*-PPS (20 mg) was dissolved in dichloromethane (0.5 mL) and was added in a dropwise manner to stirring distilled water (2 mL). The solution was stirred at room temperature until the organic solvent phase was completely removed, at which point the aqueous phase contained the formed polymeric micelles. When needed the complete evaporation was obtained under vacuum.

(b) Hot water suspension method: PEG-*b*-PPS (20 mg) was suspended directly in hot water under stirring, keeping the temperature at 60 °C until the solid polymer self-assembled and formed a micelle suspension.

The mean diameter and polydispersity of self-assembled structures in aqueous media were defined by dynamic light scattering (DLS, Zetasizer Nano ZS, Malvern Instrument Ltd., U.K.), with the concentration of the polymers at 10 mg/mL.

Cryo-transmission electron microscopy (cryo-TEM) was used to investigate the morphology of the PEG-*b*-PPS aggregates in water. The specimens for analysis were prepared by application of a drop of the aqueous aggregate suspension on a microcopper grid coated with a porous

carbon film. Excess suspension was blotted away, resulting in a 30–100 nm thick film that spans the holes of porous carbon support. The sample was then rapidly vitrified by immersion in liquid ethane, transferred to the cryo-electron microscope (Philips CM12 FEI, Eindhoven, The Netherlands) operating at 80 kV in transmission mode at a temperature never exceeding -160°C . Images were recorded on a CCD camera with minimum electron dose at a nominal magnification of up to $35000\times$.

A fluorescence probe technique, using the well-characterized pyrene²⁷ method, was used to evaluate the copolymer concentration at which the association first takes place, known as the CAC. Pyrene changes its fluorescence emission spectrum in response to the polarity of its environment.²⁸ The solvent polarity dependence of pyrene's emission is expressed in terms of the ratio I_1/I_3 , which are the intensities of bands I and III corresponding to $S_1^{n=0} \rightarrow S_0^{n=0}$ (0–0) and $S_1^{n=0} \rightarrow S_0^{n=1}$ (0–1) transitions, respectively, S_1 and S_0 being first singlet excited state and ground state, respectively. At constant pyrene concentration, the CAC of an amphiphile is obtained as the amphiphile concentration at which I_1/I_3 sharply decreases, reflecting the preferential solubilization of pyrene in a hydrophobic environment. Steady state fluorescence spectra were recorded at 25°C using a Safire² (TECAN) spectrofluorimeter. A given volume of a pyrene (98%, Aldrich) stock solution in ethanol (2×10^{-3} M) was added to the aggregate suspension such that the final pyrene concentration was 2×10^{-6} M and the mixture was stirred and left to equilibrate before performing the measurement. The excitation wavelength was fixed at $\lambda = 335$ nm, and the monomer emission was read at $\lambda = 377$ (I_1) and $\lambda = 386$ (I_3).

Encapsulation of CsA in PEG-*b*-PPS Micelles. The cosolvent evaporation method and the hot water suspension method were both used to prepare CsA-loaded polymeric micelles:

(a) PEG-*b*-PPS block copolymer (20 mg) and CsA (different ratios) were dissolved together in dichloromethane (0.5 mL), and the solution was added to 2 mL of distilled water in a dropwise manner. The organic solvent was evaporated after 2 h of stirring at room temperature (vacuum was applied to ensure the complete removal).

(b) CsA (different amounts) was previously dissolved into 20 mg of PEG-*b*-PPS block copolymer heated up to 60°C , then the mixture was suspended in 2 mL of hot water (60°C) and the suspension was kept at 60°C stirring for 2 h.

The obtained micellar solutions in both cases were centrifuged at 11,000 rpm for 10 min to remove any CsA precipitates. The size of the CsA-loaded micelles was measured by dynamic light scattering as described above.

Determination of CsA levels by GPC–UV. An amount of the CsA-loaded micelle suspension was freeze-dried and then redissolved in THF. Twenty microliters of the sample was injected in the GPC column (described above) to quantitatively separate the PEG-*b*-PPS block copolymer from the CsA. CsA concentrations were estimated by UV detection at 210 nm (photodiode array detector, WATERS 996). For each sample containing CsA and PEG-*b*-PPS analyzed by GPC–UV, a sample containing only CsA directly dissolved in THF was also injected as reference containing a CsA weight the same as the initial CsA level added to the block-copolymer. Multiple measurements were taken and averaged. Mean and standard deviation (SD) are reported. CsA encapsulation efficiency was calculated as follows: encapsulation efficiency (%) = (amount of loaded CsA)/(amount of added CsA) $\times 100\%$. Loading was calculated as follows: CsA loading (w/w) = (amount of loaded CsA)/(amount of polymer).

Determination of CsA Solubility in PPS. To determine whether CsA was soluble in PPS and thus would likely exist in solution within the PPS micelle cores, differential scanning calorimetry (DSC) was performed on CsA and on CsA putatively dissolved in PPS homopolymer (DP = 40), without the aid of any other solvent. Eight milligrams of solid CsA was analyzed by a Mettler Toledo DSC 25. The same amount of drug was first mixed with 40 mg of PPS₄₀ and then analyzed by DSC. Data obtained by both of the experiments were then compared.

Spontaneous CsA Release from PEG-*b*-PPS Micelles in Vitro. Two milliliters of freshly prepared CsA-loaded micelles was placed in a Spectro/Por dialysis bag (MWCO = 6000–8000 Da), which was incubated in 200 mL of stirred distilled water at 37°C . Samples of 100 μL were taken from the dialysis bag, and the aqueous media was refreshed every 24 h. Each sample was treated as described before for the determination of CsA concentration, from which the percentage of released drug was calculated.

Results

PEG-*b*-PPS block copolymers were synthesized by living anionic polymerization of propylene sulfide upon a PEG macroinitiator, formed by deprotection of a PEG thioacetate, similarly as previously described by our group.²⁶ In the present case, the polymerization reaction was stopped by introduction of 2,2'-dithiodipyridine as an end-capping agent (Figure 2A), which forms a disulfide bond at the PPS terminus, as might be useful for an eventual functionalization at the copolymer's end.

In this study, PEG of molecular weight 2000 g mol^{-1} (DP 44) was copolymerized with propylene sulfide blocks of nominal DP of 10, 20 and 40. Both GPC and ^1H NMR were used to characterize the block copolymers for their average molecular weights, and PEG-*b*-PPS with approximate molecular weights of 2800, 3500 and 5200 g mol^{-1} were obtained (Table 1). The PEG/PPS ratio was calculated by comparing the integral peak area of PPS methyl group protons to that of PEG methoxy group protons from the ^1H

(27) Kalyanasundaram, K.; Thomas, J. K. Environmental effects on vibronic band intensities in pyrene monomer fluorescence and their application in studies of micellar systems. *J. Am. Chem. Soc.* **1977**, *99*, 2039–2044.

(28) Winnik, F. M.; Regismond, S. T. A. Fluorescence methods in the study of the interactions of surfactants with polymers. *Colloids Surf., A* **1996**, *118*, 1–39.

Table 1. PEG-*b*-PPS Copolymers Synthesized

polymer	PS units ^a	M_n^b	M_n^c	f_{PEG} (PEG M_w/M_n^c)	polydispersity M_w/M_n^b
PEG ₄₄ - <i>b</i> -PPS ₁₀	10	3086	2800	0.73	1.06
PEG ₄₄ - <i>b</i> -PPS ₂₀	20	4356	3500	0.57	1.12
PEG ₄₄ - <i>b</i> -PPS ₄₀	40	5830	5200	0.39	1.12

^a In the feed. ^b Determined by GPC. ^c Determined by ¹H NMR.

Table 2. PEG-*b*-PPS Aggregates Formed by the Cosolvent Evaporation Method

polymer	mean aggregate size (nm) ^a	mean aggregate size (nm) ^b	aggregate morphology ^b	CAC (mg/mL)	polydispersity index
PEG ₄₄ - <i>b</i> -PPS ₁₀	14	7	Sm ^c	0.392	0.165
PEG ₄₄ - <i>b</i> -PPS ₂₀	20	13	Sm ^c	0.350	0.178
PEG ₄₄ - <i>b</i> -PPS ₄₀	22–150 ^d	22–170 ^d	Cm–V ^c	0.052	0.170

^a Determined by dynamic light scattering. ^b Determined by cryo-TEM. ^c Sm: Spherical micelles. Cm: Cylindrical micelles (wormlike). V: Vesicles. ^d We place no quantitative interpretation on the higher number; a spherical model was employed in the DLS analysis, and the large number merely suggests the presence of another mesophase, such as wormlike micelles, as was determined by cryo-TEM.

NMR (Table 1). Block copolymer polydispersity was also shown by GPC to be relatively narrow, indicating the presence of only diblock copolymers (Table 1).

We synthesized PEG-*b*-PPS with different mass fractions of PEG f_{PEG} in view of the different mesophases structures that might be so formed, i.e. different micelle sizes and shapes. Work in our laboratory has demonstrated that PEG-*b*-PPS can self-assemble in aqueous solution into vesicles, wormlike micelles and spherical micelles, as the f_{PEG} value ranges from 0.20 to 0.30, from 0.30 to 0.42, and from 0.42 to 0.75, respectively (unpublished results). In the present work, block copolymers were synthesized using amounts of propylene sulfide to give f_{PEG} values of about 0.35–0.75.

PEG₄₄-*b*-PPS₁₀, PEG₄₄-*b*-PPS₂₀ and PEG₄₄-*b*-PPS₄₀ formed self-assembled aggregates in aqueous suspension. Average diameter was measured by dynamic light scattering for the copolymer aggregates and was found to be around 14 and 20 nm for PEG₄₄-*b*-PPS₁₀ and PEG₄₄-*b*-PPS₂₀ aggregates, respectively, obtained by cosolvent evaporation (Table 2). A narrow size distribution (not shown) suggests the formation of only spherical micelles in aqueous suspension for these two copolymers, both in the presence and in the absence of CsA. This was confirmed by cryo-TEM (Figure 3A,B, Figure 4A,B). Fairly uniform dark spheres represent the PPS micellar cores, embedded in a light water matrix. The coronal domains consisting of the hydrated PEG chains provide only a marginal contrast and appear as faint haloes surrounding the micelle core. The more-or-less regular spacing between the micellar cores is indicative of the thickness of the PEG corona, or rather twice that thickness (bars in Figure 3B). The sizes of the micelles as determined by cryo-TEM (as a measurement of the core diameter only) are somewhat smaller than those determined by dynamic light scattering, namely 7 nm at f_{PEG} 0.73 (PEG₄₄-*b*-PPS₁₀) and 13 nm at f_{PEG} 0.57 (PEG₄₄-*b*-PPS₂₀) (Table 2); these measurements demonstrate the effect of hydrophobe block length on aggregate size.

Results of dynamic light scattering of aggregates formed at f_{PEG} 0.39 (PEG₄₄-*b*-PPS₄₀) were inconsistent with a spherical model, which suggested a dimension of 22 nm but also a larger length scale of 150 nm (Table 2); this result suggested the presence of wormlike micelles. Indeed, this

was confirmed by cryo-TEM, which showed a majority of wormlike micelles both in the presence and in the absence of CsA, as well as the presence of a smaller fraction of vesicles (Figure 3C,D, Figure 4C). The regular spacing of the wormlike micelles visible in Figure 3C is indicative of the diameter of the micelles, inclusive of corona thickness, with an average cross-sectional diameter of 22 nm. As visible in Figure 3C,D, a smaller fraction of vesicles were also present, having a bilayer thickness of approximately 10 nm (estimated from the images).

The pyrene method^{27–29} was used to determine the CAC of the three block copolymers synthesized and corresponded to about 0.392 mg/mL, 0.350 mg/mL and 0.052 mg/mL for PPS block lengths of 10, 20 and 40, respectively (Table 2 and Figure 5). The process of PEG-*b*-PPS block copolymer aggregation in water as measured by changes in the fluorescence intensity ratio I_1/I_3 of pyrene has been discussed in a previous work.³⁰ At constant pyrene concentration the CAC of an amphiphile is obtained as the amphiphile concentration at which I_1/I_3 sharply decreases, reflecting the preferential solubilization of pyrene in a hydrophobic environment.³¹ The I_1/I_3 values generally range from 1.87 in water to 0.6 in aliphatic hydrocarbon solvents.²⁷ Values of 1.1–1.2 are typical of simple aqueous micelles, implying that pyrene is located in the surface region of the micelle hydrocarbon core.³² For PEG-*b*-PPS block copolymers it has been observed that this ratio dropped sharply above a certain polymer concentration, corresponding to the onset of copolymer aggregation. The association transition appeared to

- (29) Winnik, F. M. Photophysics of preassociated pyrenes in aqueous polymer-solutions and in other organized media. *Chem. Rev.* **1993**, 93, 587–614.
- (30) Cerritelli, S.; Fontana, A.; Velluto, D.; Adrian, M.; Dubochet, J.; De Maria, P.; Hubbell, J. A. Thermodynamic and kinetic effects in the aggregation behavior of a poly(ethylene glycol-*b*-propylene sulfide-*b*-ethylene glycol) ABA triblock copolymer. *Macromolecules* **2005**, 38, 7845–7851.
- (31) Zhao, C. L.; Winnik, M. A.; Riess, G.; Croucher, M. D. Fluorescence probe techniques used to study micelle formation in water-soluble block copolymers. *Langmuir* **1990**, 6, 514–516.
- (32) Wang, Y. C.; Winnik, M. A. Onset of aggregation for water-soluble polymeric associative thickeners - a fluorescence study. *Langmuir* **1990**, 6, 1437–1439.

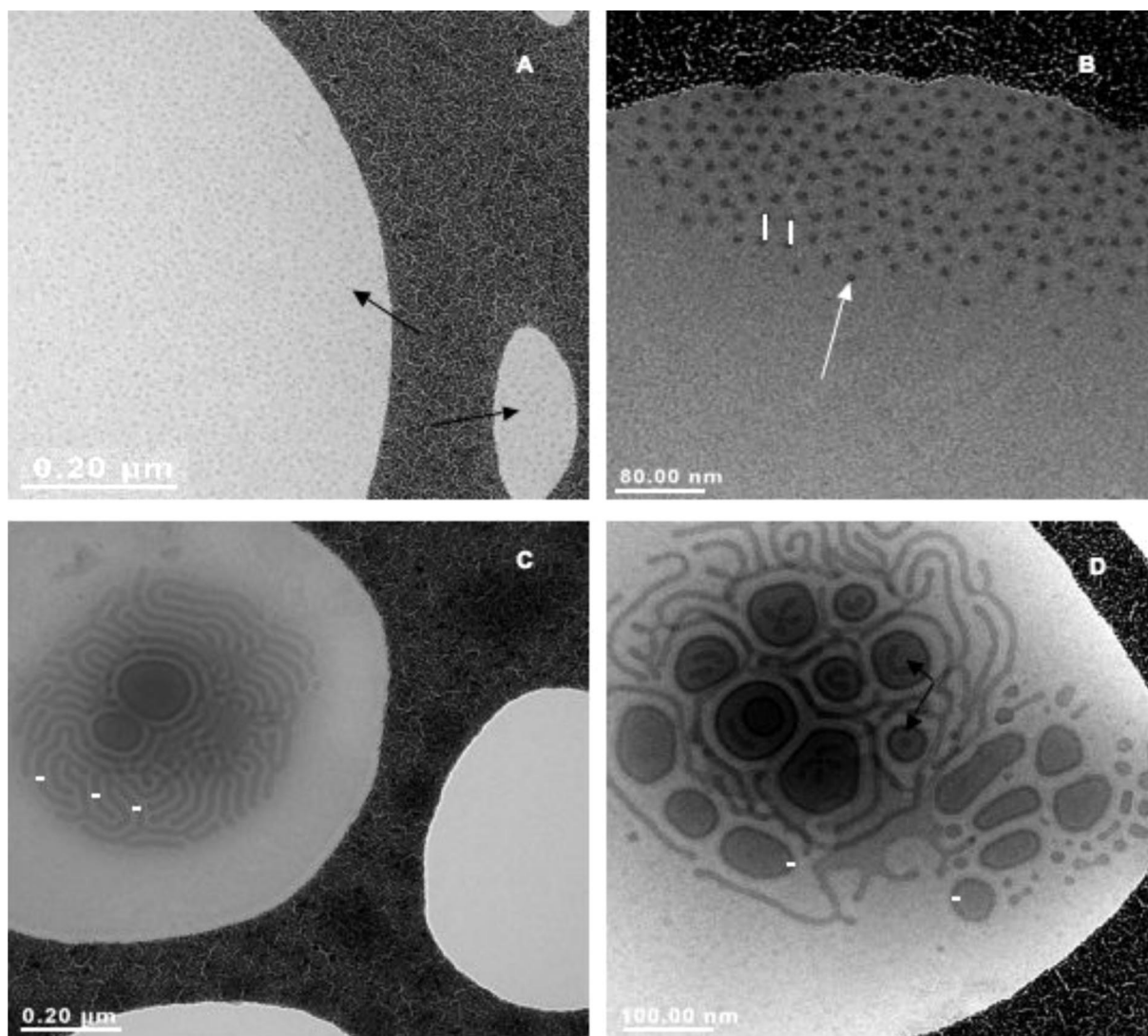


Figure 3. Cryo-TEM micrographs obtained from 1 wt % aqueous suspension of PEG₄₄-PPS₁₀ (A) or PEG₄₄-*b*-PPS₂₀ (B), or from 0.5 wt % aqueous suspensions of PEG₄₄-*b*-PPS₄₀ (C, D). In the samples of PEG₄₄-PPS₁₀ and PEG₄₄-*b*-PPS₂₀, only spherical micelles were observed (small dark spots marked by the black arrows in A and white arrows in B). The regular distance between PPS cores is indicative of the PEG corona thickness, twice this thickness being indicated by the bars in B, for example. For samples of PEG₄₄-PPS₄₀, wormlike micelles were observed (C and D), with a cross-section diameter of 22 nm (white bars in C), as well as vesicles and even vesicles containing micelles (in D). From these and additional images, the thickness of the vesicle bilayer was estimated around 10 nm.

be very broad, spanning almost a 100-fold range in polymer concentration. The final obtained I_1/I_3 value was between 1.01–1.08, indicating that PEG-*b*-PPS micelles had a highly hydrophobic core, the polarity of which is comparable to the aliphatic hydrocarbon solvents.³³

Solubility of CsA in PPS and Encapsulation Efficiency and CsA Loading in PEG-*b*-PPS Micelles. An aspect of our design was to employ the PPS core of the PEG-*b*-PPS micelles as a bona fide solvent for the hydrophobic drug, here CsA. To explore this, we performed DSC on CsA mixtures in PPS homopolymer. As expected, a clear melting transition was observed for CsA at around 130 °C; in

demonstration of the solubility of the drug in the PPS block, no such melting transition was observed for CsA in PPS at 20% w/w.

CsA was encapsulated in the copolymer aggregates simply adding the drug to the copolymer before the self-assembly process, as described in Materials and Methods. The amount of encapsulated CsA was measured by GPC after destroying the aggregate structure by freeze-drying followed by dissolution in organic solvent (THF, which dissolves both the PEG and the PPS blocks). Experiments were performed with multiple CsA/polymer weight ratios, and selected conditions are reported in Table 3 (for the cosolvent evaporation method) and Table 4 (for the hot water method).

In terms of the overall goal of solubilization of CsA, drug levels reached 1.915 mg/mL (CsA/polymer weight ratio of

(33) Dong, D. C.; Winnik, M. A. The py scale of solvent polarities. *Can. J. Chem.* **1984**, *62*, 2560–2565.

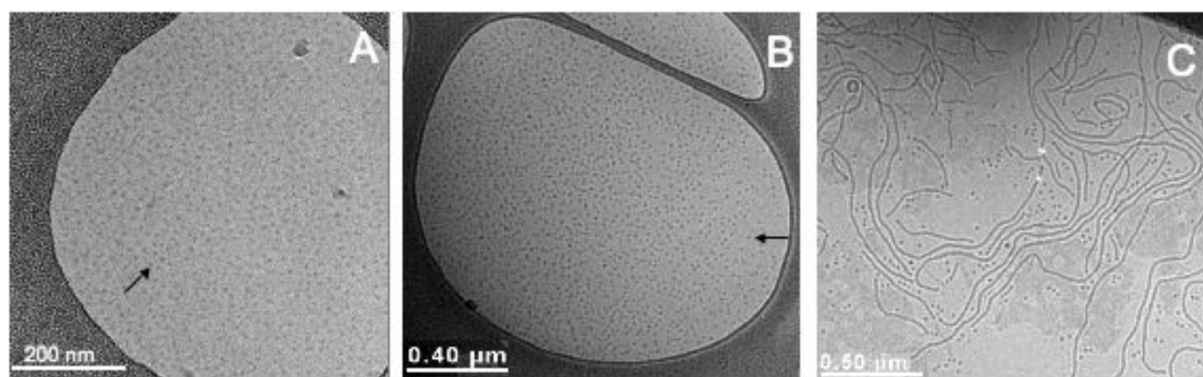


Figure 4. Cryo-TEM micrographs obtained from 1 wt % aqueous suspension of loaded CsA PEG₄₄-*b*-PPS₁₀ (A) or PEG₄₄-*b*-PPS₂₀ (B), or from 0.5 wt % aqueous suspensions of loaded CsA PEG₄₄-*b*-PPS₄₀ (C). In the samples of PEG₄₄-*b*-PPS₁₀ and PEG₄₄-*b*-PPS₂₀, only spherical micelles were observed. For samples of PEG₄₄-*b*-PPS₄₀, wormlike micelles were observed. The presence of the drug within the hydrophobic core of the micelles influences neither their size nor their shape.

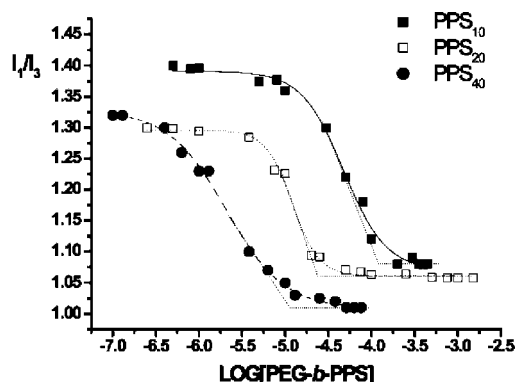


Figure 5. Plot of the fluorescence intensity ratio I_1/I_3 as a function of the concentration of PEG₄₄-*b*-PPS₁₀ (filled squares), PEG₄₄-*b*-PPS₂₀ (open squares) and PEG₄₄-*b*-PPS₄₀ (filled circles). The samples were prepared by the cosolvent evaporation method and dilution in water.

0.1915) in aqueous suspension in the presence of PEG-*b*-PPS micelles and vesicles under the encapsulation conditions used. Considering that only 23 μg of CsA may be solubilized in 1 mL of water, this corresponds to an effective CsA water solubility increase of almost 10^3 -fold by use of the PEG-*b*-PPS micelles at a polymer concentration of 10 mg/mL. Clearly, at higher polymer micelle concentrations, even higher CsA effective solubilities can be obtained.

Results reported in Table 3 and in Figure 6 show that, using the cosolvent evaporation method, achievable loadings depended strongly on the DP of the PPS block, while loading efficiency did not. Many more experiments were performed than are reported in this table, in which the ratio of CsA/polymer was also varied at constant copolymer architecture. Only those ratios that were near the maximum loading are reported, corresponding to ratios of from 1.0 to 1.5 mg of CsA per 20 mg of copolymer for PEG₄₄-*b*-PPS₁₀, 4.0 mg for PEG₄₄-*b*-PPS₂₀, and 6.0 mg for PEG₄₄-*b*-PPS₄₀. For the highest PPS block length, a loading of 0.19 mg of CsA per mg of copolymer was achieved. The CsA loaded aggregates were the same size and shape as drug-free aggregates (Table 3).

Similar results were obtained with the hot water suspension method (Table 4), which yielded a maximum effective solubility of 1.13 mg/mL CsA at a polymer concentration of 10 mg/mL. For the spherical micelle-forming compositions of PEG₄₄-*b*-PPS₁₀ and PEG₄₄-*b*-PPS₂₀, loading and encapsulation efficiencies were similar as achieved with the cosolvent evaporation method. Likewise, spherical micelle size was close to the same and independent of CsA loading (Table 4). At the highest PPS block length of DP 40, however, which forms wormlike micelles and vesicles, the hot water suspension method failed, leading to low loading and low encapsulation efficiency. This may be related to the higher viscosity of the longer PPS domains.

Spontaneous CsA Release from PEG-*b*-PPS Vesicles in Vitro. The release of micelle-encapsulated CsA was measured in vitro as a function of PPS block length. Release was observed to be more-or-less linear in time and sustained over 9–12 days at 37 °C for the molecular formulations evaluated, ca. 9 days for the shortest PPS block length and ca. 12 days for the middle and longer PPS block length (Figure 7). These long release times surely support the assumption that diffusion through the employed dialysis membrane was rapid (its MWCO is 6000–8000 g mol⁻¹) relative to the overall release rate. It was observed that there was only a minor dependence in release rate upon spherical micelle size (contrasting release from PEG₄₄-*b*-PPS₁₀ vs PEG₄₄-*b*-PPS₂₀; $P < 0.01$ for comparison of the slopes of the linear fit between the curves, based on the hypothesis that the PPS₁₀-containing polymer releases statistically faster) and no dependence upon micelle shape (comparing release from PEG₄₄-*b*-PPS₂₀ vs PEG₄₄-*b*-PPS₄₀; $P > 0.7$). This stands to reason: in all cases, the diffusion length scales are very small, and the release rate seems to depend rather upon the partitioning of the CsA from the hydrophobic PPS phase into water.

Discussion

Although CsA is currently one of the most widely used immunosuppressive drugs, it requires rigorous monitoring,

Table 3. PEG-*b*-PPS Aggregates Formed by the Cosolvent Evaporation Method

polymer	CsA added (mg) ^a	CsA loading, mean ± SD (mg/mg)	encapsulation efficiency, mean ± SD (%)	mean aggregate size (nm) ^b	mean aggregate size (nm) ^c
PEG ₄₄ - <i>b</i> -PPS ₁₀	1	0.0305 ± 0.002	60.9 ± 4.1	14	10
PEG ₄₄ - <i>b</i> -PPS ₂₀	4	0.1300 ± 0.030	66.0 ± 7.3	21	17
PEG ₄₄ - <i>b</i> -PPS ₄₀	6	0.1915 ± 0.030	63.8 ± 9.2	148	20 ^d

^a Per 20 mg of copolymer. ^b Determined by dynamic light scattering. ^c Determined by cryo-TEM. ^d Value measured for the diameter of the cylindrical micelles.

Table 4. PEG-*b*-PPS Aggregates Formed by the Hot Water Suspension Method

polymer	CsA added (mg) ^a	CsA loading, mean ± SD (mg/mg)	encapsulation efficiency, mean ± SD (%)	mean aggregate size (nm) ^b
PEG ₄₄ - <i>b</i> -PPS ₁₀	1.5	0.0545 ± 0.006	73.0 ± 8.8	14
PEG ₄₄ - <i>b</i> -PPS ₂₀	4	0.1130 ± 0.020	56.3 ± 8.1	24
PEG ₄₄ - <i>b</i> -PPS ₄₀	6	0.0308 ± 0.030	15.4 ± 2.5	190

^a Per 20 mg of copolymer. ^b Determined by dynamic light scattering.

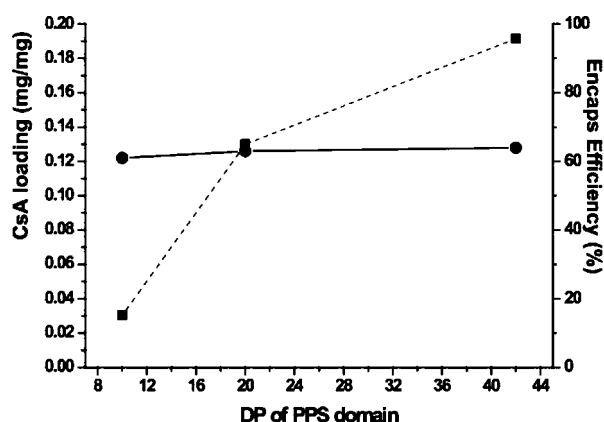


Figure 6. CsA loading and encapsulation efficiency are shown as a function of PPS block DP for the cosolvent encapsulation method. CsA loading depended strongly upon PPS block DP, while loading efficiency did not.

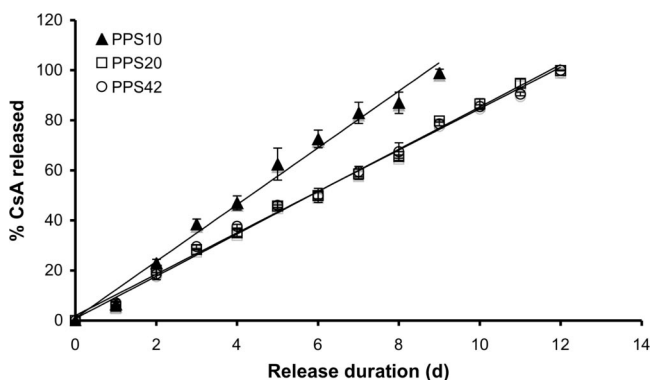


Figure 7. In vitro release of CsA at 37 °C from PEG-*b*-PPS micelles showed a modest dependence upon PPS DP and thus aggregate size (contrast PEG₄₄-*b*-PPS₁₀ with PEG₄₄-*b*-PPS₂₀), but not aggregate morphology (compare PEG₄₄-*b*-PPS₂₀ with PEG₄₄-*b*-PPS₄₀).

since there is a poor correlation between administered dose and clinical response, which may relate to large intersubject variability in bioavailability and metabolism of the drug.³⁴ The therapeutic window is narrow, and the consequences of therapeutic and toxic levels are severe graft rejection on one

hand and nephrotoxicity on the other.³⁵ It has been also reported that Cremophor EL, the solubilizing agent present used in the commercially available intravenous dosage form of CsA, is nephrotoxic and hemolytic.³⁶ Such complexities are not unique to CsA: it is merely one example of many of a poorly water-soluble drug with a pharmacological profile that is correspondingly complicated. From the perspective of an example of a poorly soluble drug, it is perhaps a difficult example, due to its high molecular weight peptide structure.

In the present study, we sought to explore the potential of PEG-*b*-PPS micelles and vesicles to solubilize and retain CsA using in vitro models. As to the components, we selected the hydrophilic block PEG based on a large literature in biomaterial passivation,^{12,37,38} nanoparticle passivation^{39,40} and delay of protein clearance after PEG grafting.^{41–43} Our laboratory has explored PPS as an oxidation-sensitive, low glass transition temperature hydrophobic polymer that can

- (34) Curtis, J. J. Experience with cyclosporine. *Transplant. Proc.* **2004**, *36*, 54S–58S.
- (35) Curtis, J. J. Posttransplant hypertension. *Transplant. Proc.* **1998**, *30*, 2009–2011.
- (36) Tibell, A.; Larsson, M.; Alvestrand, A. Dissolving intravenous cyclosporine-a in a fat emulsion carrier prevents acute renal side-effects in the rat. *Transplant Int.* **1993**, *6*, 69–72.
- (37) Peppas, N. A.; Langer, R. New challenges in biomaterials. *Science* **1994**, *263*, 1715–1720.
- (38) Tessmar, J. K.; Gopferich, A. M. Customized peg-derived copolymers for tissue-engineering applications. *Macromol. Biosci.* **2007**, *7*, 23–39.
- (39) Peracchia, M. T.; Fattal, E.; Desmaele, D.; Besnard, M.; Noel, J. P.; Gomis, J. M.; Appel, M.; d'Angelo, J.; Couvreur, P. Stealth PEGylated polycyanoacrylate nanoparticles for intravenous administration and splenic targeting. *J. Controlled Release* **1999**, *60*, 121–128.
- (40) Yoncheva, K.; Lizarraga, E.; Irache, J. M. PEGylated nanoparticles based on poly(methyl vinyl ether-co-maleic anhydride): Preparation and evaluation of their bioadhesive properties. *Eur. J. Pharm. Sci.* **2005**, *24*, 411–419.
- (41) Bearinger, J. P.; Terrettaz, S.; Michel, R.; Tirelli, N.; Vogel, H.; Textor, M.; Hubbell, J. A. Chemisorbed poly(propylene sulphide)-based copolymers resist biomolecular interactions. *Nat. Mater.* **2003**, *2*, 259–264.

be converted into a water-soluble polymer by oxidation, providing a potential pathway for clearance from the body as a soluble polymer.^{21,44} Because PEG is water-soluble, while PPS is strongly water-insoluble, self-assembled mesophases are expected in water, and micelles, wormlike micelles and vesicles have been observed.^{23,30} The amorphous nature of the hydrophobic core, well above its T_g , enables high drug loading, and in the case of CsA the core even serves as a bona fide solvent for the drug.

The anionic living polymerization employed enabled well-defined, low polydispersity AB block copolymers to be formed.²⁶ This, in turn, enabled well-defined studies to be conducted to correlate PEG-*b*-PPS architecture to mesophase structure (morphology and size). In doing so, we observed that PEG₄₄-*b*-PPS₁₀ and PEG₄₄-*b*-PPS₂₀ formed only spherical micelles, while PEG₄₄-*b*-PPS₄₂ formed wormlike micelles and, to an extent, vesicles. The structure of the self-assemblies could be quite reasonably rationalized based on the copolymer hydrophilic fraction f_{PEG} .⁴⁵

One limitation in the practical use of polymer micelles in clinical formulations is the loading that can be achieved. In this regard, we were quite pleased to be able to achieve up to 0.19 mg of CsA per mg of copolymer for the highest PPS block length examined. A dependence upon PPS block length was observed, with, quite reasonably, higher PPS molecular mass fractions leading to higher loadings: since the PEG domain carries no drug, but the PEG molecular mass accounts also to the total molecular mass, this dependence is expectable. With PEG₄₄-*b*-PPS₄₀, an increase in overall effective CsA solubility of 10³-fold could be achieved, at a polymer concentration of 10 mg/mL. This is within a range that is clinically interesting.

A second limitation in the practical use of polymer micelles in clinical formulations is the encapsulation efficiency that can be achieved. In this regard also, we were pleased to be able to achieve encapsulation efficiencies approaching 70%. Clearly, even higher encapsulation efficiencies would be desirable, but this attained value is also within the range of acceptability for a commercially interesting pharmaceutical process.

Finally, the typical complexity of drug encapsulation within block copolymers to form micelles is not insignificant.

While the cosolvent evaporation method is commercializable, a method so simple as suspending a drug-containing polymer in hot water could have distinct advantages, lacking any issues of vacuum processing to remove organic solvents. In this regard, we were very pleased with the results obtained with PEG₄₄-*b*-PPS₂₀, which showed loading to 0.11 mg CsA/mg copolymer at an encapsulation efficiency of almost 60% to yield spherical micelles 24 nm in diameter. The hot water suspension method failed with PEG-*b*-PPS with a block DP of 40. Clearly, somewhere between a DP of 20 and a DP of 40 lies the maximum PPS block length processable by the hot water suspension method.

Because of the hydrophobicity of the PPS block, the CACs of the PEG-*b*-PPS block copolymers were low and the assemblies that were formed were correspondingly stable.⁴⁶ In some assemblies, the mobility of the hydrophobic domains can be so low that the core can be considered to be totally frozen.³⁰ This, in turn, can lead to prolonged release of the hydrophobic drug under sink conditions, as we observed for the PEG-*b*-PPS copolymers investigated. Release over periods of 9–12 days was observed, with the very small core assemblies (from PEG₄₄-*b*-PPS₁₀) releasing only slightly faster than larger core assemblies (for example, from PEG₄₄-*b*-PPS₂₀). Even though the hydrophobic domain exists well above its T_g , the prolonged drug release rate clearly demonstrates a slow rate of micelle dissociation upon dilution.

A number of block copolymer systems have been investigated for polymer micelles, and some have been explored for CsA solubilization and release. It is interesting to compare our results with these.^{9,46–48} First, such high CsA loading values have not been achieved, and this may be due to the high compatibility between the drug and PPS block which forms the core of the micelles. Many studies have indicated that the major factor influencing both the loading capacity and the loading efficiency of block copolymer micelles is the compatibility between the solubilize and core-forming block.³ Because of its high hydrophobicity, the PPS block can easily solubilize the CsA by mean of hydrophobic interactions, as was demonstrated by DSC of CsA mixed within PPS homopolymer, which showed a complete lack of any CsA melting transition.

Second, the encapsulation efficiency that was attainable with PEG-*b*-PPS seems favorable by comparison of these results with what has been previously reported on the CsA loading into micelles, nanoparticles and liposomes.⁴⁹ Micelles

- (42) Kataoka, K.; Matsumoto, T.; Yokoyama, M.; Okano, T.; Sakurai, Y.; Fukushima, S.; Okamoto, K.; Kwon, G. S. Doxorubicin-loaded poly(ethylene glycol)-poly(beta-benzyl-L-aspartate) copolymer micelles: Their pharmaceutical characteristics and biological significance. *J. Controlled Release* **2000**, *64*, 143–153.
- (43) Tosatti, S.; De Paul, S. M.; Askendal, A.; VandeVondele, S.; Hubbell, J. A.; Tengvall, P.; Textor, M. Peptide functionalized poly(L-lysine)-g-poly(ethylene glycol) on titanium: Resistance to protein adsorption in full heparinized human blood plasma. *Biomaterials* **2003**, *24*, 4949–4958.
- (44) Rehor, A.; Hubbell, J. A.; Tirelli, N. Oxidation-sensitive polymeric nanoparticles. *Langmuir* **2005**, *21*, 411–417.
- (45) Cerritelli, S.; O'Neal, C.; Fontana, A.; Adrian, M.; Dubochet, J.; Hubbell, J. A. Poly(ethylene glycol-bi-propylene sulfide) di- and triblock copolymers: Aggregation behavior in aqueous solution. Manuscript in preparation.

- (46) Francis, M. F.; Lavoie, L.; Winnik, F. M.; Leroux, J. C. Solubilization of cyclosporin a in dextran-g-polyethyleneglycol-alkyl ether polymeric micelles. *Eur. J. Pharm. Biopharm.* **2003**, *56*, 337–346.
- (47) Aliabadi, H. M.; Elhasi, S.; Mahmud, A.; Gulamhusein, R.; Mahdipoor, P.; Lavasanifar, A. Encapsulation of hydrophobic drugs in polymeric micelles through co-solvent evaporation: The effect of solvent composition on micellar properties and drug loading. *Int. J. Pharm.* **2007**, *329*, 158–165.
- (48) Lee, M. K.; Choi, L.; Kim, M. H.; Kim, C. K. Pharmacokinetics and organ distribution of cyclosporin a incorporated in liposomes and mixed micelles. *Int. J. Pharm.* **1999**, *191*, 87–93.

formed by modified polysaccharides are able to load up to 8.5% of CsA.⁵⁰ Nanoparticles made of polycaprolactone (PCL) and polystearic acid (PSA) have been investigated by Molpeceres⁵¹ and Valera⁵² and by Zhang⁵³ respectively, and they showed loading up to 13% CsA w/w (PCL) or 2.5% w/w (PSA). The use of liposomes has been also considered, and CsA has been incorporated up to 3.0% w/w, while mixed micelles of dimyristoyl phosphatidyl choline and distearoyl phosphoethanolaminepolyethylene glycol 2000 loaded 6% w/w of CsA.⁴⁸ Incorporation of CsA into poly(ethylene glycol)-*b*-poly(ϵ -caprolactone) micelles has been recently reported,⁹ showing loading up to 13% w/w, close to the levels achieved here.

-
- (49) Beauchesne, P. R.; Chung, N. S. C.; Wasan, K. M. Cyclosporine a: A review of current oral and intravenous delivery systems. *Drug Dev. Ind. Pharm.* **2007**, *33*, 211–220.
- (50) Francis, M. F.; Cristea, M.; Yang, Y. L.; Winnik, F. M. Engineering polysaccharide-based polymeric micelles to enhance permeability of cyclosporin A across caco-2 cells. *Pharm. Res.* **2005**, *22*, 209–219.
- (51) Molpeceres, J.; Aberturas, M. R.; Guzman, M. Biodegradable nanoparticles as a delivery system for cyclosporine: Preparation and characterization. *J. Microencapsulation* **2000**, *17*, 599–614.
- (52) Varela, M. C.; Guzman, M.; Molpeceres, J.; Aberturas, M. D.; Rodriguez-Puyol, D.; Rodriguez-Puyol, M. Cyclosporine-loaded polycaprolactone nanoparticles: Immunosuppression and nephrotoxicity in rats. *Eur. J. Pharm. Sci.* **2001**, *12*, 471–478.
- (53) Zhang, Q. N.; Yie, G. Q.; Li, Y.; Yang, Q. S.; Nagai, Y. T. Studies on the cyclosporin a loaded stearic acid nanoparticles. *Int. J. Pharm.* **2000**, *200*, 153–159.

In addition, in terms of encapsulation methodology, the hot water suspension method would appear to be very favorable from a process perspective compared to what has been presented in the literature for CsA. It may be that the low glass transition temperature of the PPS block and low melting temperature of the block copolymer enable the use of such a simple drug encapsulation approach.

While delayed release of CsA from block copolymer micelles may be clinically less important than achieving high effective solubility, it is nevertheless interesting in terms of providing more constant drug concentrations between dosage administrations as well as more convenient dosage regimens. In this regard, the relatively linear release of CsA observed from the PEG-*b*-PPS micelles over time, for all block copolymer architectures investigated, is interesting. Delayed release from poly(ethylene glycol)-*b*-poly(ϵ -caprolactone) micelles has been demonstrated as well, retaining the 94% of their drug content after 12 h, while Cremophor EL micelles have been shown to release 77% of their drug content by 12 h.⁹

Given the ease and efficiency with which the PEG-*b*-PPS diblock copolymer micelles may be loaded, the high load of bona fide soluble drug that they contain, and their oxidative mechanism of degradation, we are interested in their use in a number of applications. These include cancer chemotherapy, where, as discussed above, polymer micelles may accumulate due to vascular hyperpermeability, as well as situations of surgery, when the sustained release characteristics of the materials may be particularly useful.

MP7001297